PAPER

Check for updates

Fly ash geopolymer as a coating material for controlled-release fertilizer based on granulated urea

Rashidah Mohamed Hamidi,[*a] Ahmer Ali Siyal, [ID][a] Tero Luukkonen, [ID][b] Rashid M. Shamsuddin [ID] [*a] and Muhammad Moniruzzaman [ID][c]

Nitrogen loss from urea fertiliser due to its high solubility characteristics has led to the invention of controlled release urea (CRU). Majority of existing CRU coatings are produced from a non-biodegradable, toxic and expensive synthetic polymers. This study determines the feasibility of fly ash-based geopolymer as a coating material for urea fertilizer. The effects of fly ash particle size (15.2 µm, 12.0 µm, and 8.6 µm) and solid to liquid (S : L) ratio (3 : 1, 2.8 : 1, 2.6 : 1, 2.4 : 1 and 2.2 : 1) on the geopolymer coating, the characterization such as FTIR analysis, XRD analysis, surface area and pore size analysis, setting time analysis, coating thickness, and crushing strength, and the release kinetics of geopolymer coated urea in water and soil were determined. Lower S : L ratio was beneficial in terms of workability, but it had an adverse impact on geopolymer properties where it increased porosity and decreased mechanical strength to an undesirable level for the CRU application. Geopolymer coated urea prepared from the finest fly ash fraction and lowest S : L ratio demonstrated high mechanical strength and slower urea release profile. Complete urea release was obtained in 132 minutes in water and 15 days in soil from geopolymer-coated urea whereas for uncoated urea it took only 20 minutes in water and 3 days in soil. Thus, geopolymer can potentially be used as a coating material for urea fertilizer to replace commonly used expensive and biodegradable polymer-based coatings.

1. Introduction

Sustainable development has become the main agenda in every industrial sector worldwide. The goal is to fulfill the needs of the still increasing world population without jeopardizing natural ecosystems. For instance, maintaining a secure and functioning food supply globally is one of the major challenges now. The prices of nitrogen and phosphorus fertilizers have been on the increase,[1] which has been further aggravated by the COVID-19 pandemic and Russia–Ukraine war. On the other hand, the global nitrogen cycle is the most severely disrupted planetary boundary, as defined by the Stockholm Resilience Centre.[2] In this context, controlled- and slow-release fertilizers (CRF and SRF) could be adopted as a means to reduce nitrogen and other nutrient losses by regulating and delaying their release.[3] The main difference between CRF and SRF is that the former is available in a granular form and its nutrient release is only affected by the soil temperature whereas the latter is available in granular, nuggets or packets/sachet forms and its nutrient release is affected by soil temperature, microorganisms, moisture, surface area, and pH.[4] The use of CRF or SRF could ensure the availability of nutrients for a longer time and minimise the negative impact of excessive fertilizer, such as urea release towards environment and human health.[5,6] Coated urea, a type of CRF, is readily available on the market. It is made by applying a coating film to cover the urea granules, acting as a physical barrier from the surrounding moisture.[7,8]

Various types of coating materials have been used to produce urea based CRF such as sulphur, synthetic polymers, or biopolymers.[9–12] Suherman *et al.*[13] reported that sulphur-coated urea exhibited a delayed urea release rate with 0.038 to 0.047 g s^{-1} as compared to uncoated urea release rate of 0.060 g s^{-1}. In another study, nutrient release in soil from uncoated urea was 100% while sulphur-coated urea showed ∼32% release after 7 days of application.[14] Nonetheless, the brittle nature of sulphur coating and proneness to fracture remains a major concern. Moreover, after degradation of the sulphur coating, formation of sulphuric acid takes place, which results in increase of soil acidity.[15,16] This may lead to an adverse impact towards plant species diversity and contribute to the emission of greenhouse gases, such as N$_2$O.[17] Polymer-coated urea, for example

aHICoE, Centre for Biofuel and Biochemical Research (CBBR), Institute of Self-sustainable Building, Department of Chemical Engineering, Universiti Teknologi PETRONAS, 32610 Bandar Seri Iskandar, Perak Darul Ridzuan, Malaysia. E-mail: mrashids@utp.edu.my

bUniversity of Oulu, Fibre and Particle Engineering Research Unit, P.O. Box 8000, FI-90014, Finland

cCentre of Research in Ionic Liquids (CORIL), Institute of Contaminant Management, Department of Chemical Engineering, Universiti Teknologi PETRONAS, 32610 Bandar Seri Iskandar, Perak Darul Ridzuan, Malaysia

polyurea-coated urea, displayed 0.3% urea release within 24 h,[18] whereas polyethylene-based coating material showed 3% release in 2 d.[19] Even though polymer-coated urea exhibited a profound ability to delay the release, synthetic polymers are typically non-biodegradable involving toxic and harmful chemicals as well as complex and costly production processes.[20,21] Diverting towards more sustainable material, biodegradable biopolymer-based coating was introduced in the form of lignin-coated urea. It demonstrated 43% of urea release within 24 h in distilled water.[22] Delayed release rate was also observed in starch-coated urea with 33.6% urea release compared to 79.7% from uncoated urea in 24 h.[23] Despite being eco-friendly material, lignin is expensive and requires hazardous organic solvents during preparation. Starch, on the other hand, degrades easily and has low water resistance thus limiting its ability to form a good quality coating material.[24] Therefore, in this research, the focus is to determine the feasibility of geopolymers as a new coating material for urea fertilizer.

Geopolymers are inorganic aluminosilicate materials, for which the initial terminology was introduced by Joseph Davidovits in 1978.[25,26] Geopolymers are considered as green materials since they can be produced using locally available industrial waste or by-product materials such as different fly ashes, which are produced abundantly during the combustion of coal or other solid fuels in power plants.[27–29] A large fraction of fly ashes is disposed to landfills where they might leach potentially toxic elements to soil and subsequently contaminate groundwater. In addition, the low-density particles of ashes are susceptible to be dispersed by wind, and thus polluting the air as well. Utilizing fly ashes as a value-added material in geopolymer production reduces their negative impact towards the environment, avoids land use for waste disposal sites and diminishes the reliance on primary natural resources.[30,31] Furthermore, geopolymer synthesis is a relatively fast process (few hours)[32–34] and it can be conducted at room temperature or at temperature less than 100 °C, which consumes less energy in comparison to for example synthetic zeolites or ceramics.[35] The utilization of waste as a raw material and energy saving result in low production costs, which sum up the advantages and sustainability of geopolymer. The excellent properties of geopolymers such as high early strength,[36] resistance towards aggressive chemical environment,[37,38] stability at high temperature and long-term durability[39,40] make it a prominent material in several applications. Nonetheless, the utilization of geopolymer in agricultural applications remains scarce up to now. Only few studies have been conducted on the use of geopolymer as a coating material for controlled release urea.[12,41] A study used fly ash geopolymer to double coat it on the urea granules already coated with modified starch[12] while another study used Loess based geopolymer as an inorganic material to prepare an organic/inorganic composite coating for control release urea consisting of Loess geopolymer and organic polymers (starch (Sta) and polyvinyl alcohol (PVA)).[41] However, the effect of particle size of fly ash and the solid to liquid ratio on the coating properties and performance has never been studied.

The aim of this study is to use fly ash-based geopolymer for urea granule coating. It is hypothesized that the geopolymer coating could provide both efficient mechanical protection and suitable soluble nitrogen species diffusion and water permeation characteristics to obtain desirable CRFs. The effect of particle size of fly ash and the solid to liquid ratio (S : L) of the geopolymer mix design and their effect towards the physical, mechanical, and consequently the urea release properties were investigated.

2. Experimental procedure

2.1 Materials

Fly ash was obtained from the Lumut power plant located near Lumut, Malaysia, which uses coal as a fuel. Chemical composition of fly ash is shown in Table 1. It is a class F fly ash based on its chemical composition. Analytical reagent grade NaOH was purchased from R&M Chemicals. Urea pellets (99.99%) were purchased from Petronas Fertiliser Kedah Sdn Bhd (Malaysia) with size ranging from 3.0 to 3.5 mm.

2.2 Methods

2.2.1 Mechanical activation of fly ash. Original fly ash (OFA) was subjected to pre-treatment using high energy planetary ball mill (FITSCH, Pulverisette 5 classic line). The ball mill consists of two milling slots with stainless steel jar (250 ml capacity) and 5 mm diameter stainless-steel balls as the grinding chamber and media respectively. Dry mechanical milling method was used, and the operating parameters selected are summarized in Table 2.

2.2.2 Synthesis of geopolymer. OFA, MFA A and MFA B (mechanically activated fly ash), corresponding to the particle mean size (d_{50}) of 15.2, 12.0 and 8.6 μm, respectively, were used for geopolymer synthesis. 12 M NaOH solution was prepared by dissolving desired amount of NaOH pellets in desired volume of distilled water and the solution was allowed to cool down to room temperature for about 1 hour. The solid to liquid (S : L) weight ratio (where solid refers to fly ash and liquid to NaOH solution) was varied in the range of 3.0 : 1.0 to 2.2 : 1.0 (3.0 : 1.0, 2.8 : 1.0, 2.6 : 1.0, 2.4 : 1.0 and 2.2 : 1.0) and denoted as I (3.0 : 1.0) to V (2.2 : 1.0), respectively. Geopolymer samples were prepared by mixing fly ash with 12 M NaOH solution at 425 rpm for 10 minutes using an overhead mechanical stirrer (IKA RW20

Table 1 Chemical composition of the fly ash used in the present study

Oxide	SiO$_2$	Al$_2$O$_3$	Fe$_2$O$_3$	CaO	K$_2$O	Na$_2$O	P$_2$O$_5$
Composition (wt%)	40.8	35.4	1.86	3.71	0.69	2.96	1.36

Table 2 Operational parameter of mechanical activation

Revolution speed (rpm)	Ball to powder ratio (BPR)	Residence time (min)
300	2 : 1, 3 : 1, 4 : 1, 5 : 1, 6 : 1	60

Digital). The geopolymer slurry was cured in an electric oven at 80 °C for 24 h. Geopolymer samples were ground using mortar and pestle for characterization.

2.2.3 Preparation of geopolymer coated urea. Geopolymer paste for urea coating prepared from suitable S : L ratio and different fly ash particle size (OFA, MFA A and MFA B) which used to coat the urea and yielded in geopolymer coated urea (GCU) and referred as GCU-O, GCU-MA, and GCU-MB, respectively. 150 g of urea granules were coated with fresh state geopolymer paste by means of a spraying technique using a hand spray gun with the presence of heat as shown in Fig. 1. Geopolymer paste was charged into the spray gun container, which was placed above a nozzle. Dispersion of geopolymer paste was achieved by pumping it through the nozzle with pressurized air supplied from a compressor. Coating was stopped after the urea granules were completely covered with the geopolymer paste. Then, the geopolymer coated urea (GCU) was placed in a closed container and subjected to further curing at 80 °C for 24 h. Finally, to cover the coating imperfections wax (paraffin wax, R&M Chemicals), acting as sealant was melted at 70 °C, and GCU was dipped into the molten wax and later dried at ambient temperature and produced sealed GCU.

2.2.4 Characterization. Particle size distribution as well as the specific surface area of fly ash particles were determined using a particle size analyser (Mastersizer 2000, Malvern instruments). The structural elucidation to identify functional groups and chemical bonding present in the sample was determined using Fourier transform infrared spectrometer (spectrum one FTIR, PerkinElmer). 2 mg of fly ash was mixed with 200 mg of analytical reagent grade potassium bromide (KBr, Merck, Germany) and subjected to grinding using agate mortar to prepare the pellet for FTIR analysis. The crystalline phases present in geopolymers were determined using X-ray diffraction (Bruker D8 Advanced XRD). Diffraction pattern was obtained based on the operating condition of 40 kV and 40 mA

with CuKα source of radiation ($\lambda = 1.5406$ Å) at a scanning range of 2θ angle from 5° to 70°. The specific surface area and porosity (pore size distribution and pore volume) of the sample was analysed using Micrometrics ASAP 2020. The setting time of geopolymer paste was determined using Vicat apparatus (NL 3012 X 1002). The thickness and uniformity of geopolymer film coating on the urea granules were characterized by portable digital microscope (Dino-Lite, Plus) in the magnification range from 60 to 175×. GCUs were subjected to crushing strength analysis performed by a tablet hardness tester, TBH325 ERWEKA. The coated granules were placed onto the platform and compressed by a 500 N load cell at a speed of 2.3 mm s^{-1}.

2.2.5 Urea release kinetics in water and soil. Dissolution tester DT-720, ERWEKA, was used to determine the rate of urea release. 25 g of urea granules were placed in the dissolution vessels containing 250 ml of distilled water (release medium) and covered with the vessel cover. The release test was conducted at room temperature while agitating at a constant speed of 30 rpm with the designated paddle attached to the dissolution tester. 2.5 ml of solution was taken out with intervals of 2 min and 1 h for uncoated urea and GCUs, respectively. 2.5 ml of distilled water was added each time after sampling to replace the withdrawn solution. The extracted samples were analysed by refractometer (RX-5000, Alpha, Atago).

The buried bag method was adopted for determining the release of urea from uncoated urea and GCUs into the soil.[42] 2 g of urea granules were placed in a nylon bag, sealed, and embedded in 200 g air dried soil kept in a covered plastic container 5 cm beneath the surface of the soil. Moisture content of the soil was maintained at 30% throughout the experiment by periodically adding tap water when necessary. The moisture content was determined using a moisture content analyzer (Metler Toledo, USA). The bags containing granules were collected daily. Once the bag was retrieved, the granules inside were removed and the sample surface was cleaned. The samples were then weighed and the amount of urea release was measured by the weight loss.[43] The drying at room temperature was continued until a constant weight was achieved where there was approximately no change in weight with respect to time. Release experiment for each sample was conducted in triplicate.

3. Results and discussion

3.1 Mechanical activation of fly ash

Mechanical activation was conducted to reduce the particle size of fly ash, and subsequently increase its reactivity due to enhanced surface area. During mechanical activation *via* ball milling, energy is transferred to fly ash particles. Based on the simple collision theory, the transfer of energy occurs *via* ball-powder-ball and ball-powder-wall collisions. An increase in a ball to powder ratio by weight (BPR) allows increment in the number of potential collisions to take place at a time and eventually results in high energy transfer which is responsible for particle size reduction.[3] The results obtained (Table 3) are consistent with this explanation, whereby the lowest BPR of 2 : 1 displayed a particle size of 11.9 μm and it dropped to a smaller size of 4.4 μm when the BPR was 6 : 1.
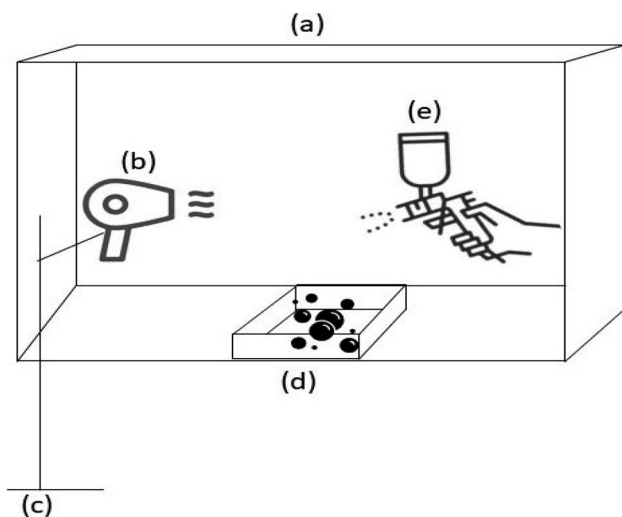

Fig. 1 Spraying chamber and set up of coating process (a) spraying chamber, (b) hair dryer, (c) retort stand, (d) sample (urea and coated urea) holder and (e) spraying gun.

Table 3 Fly ash particle size as a function of a ball to powder ratio by weight (BPR)

Residence time (min)	Revolution speed (RPM)	BPR	Particle size (µm)		
			d_{10}	d_{50}	d_{90}
60	300	2 : 1	2.264	11.953	44.348
		3 : 1	2.337	9.555	25.014
		4 : 1	2.148	8.588	21.766
		5 : 1	1.855	6.44	15.209
		6 : 1	1.259	4.449	9.89

From the mechanical activation, only few particle sizes of interest were selected to be utilised in the preparation of geopolymer. OFA, MFA A, and MFA B with the median particle sizes of 15.2 µm, 12.0 µm, and 8.6 µm respectively were the largest, medium, and smallest particle size samples. Based on the preliminary studies, mechanically activated fly ash with particle size less than 8.6 µm resulted in flash setting during geopolymer synthesis. Consequently, this particle size (<8.6 µm) of fly ash failed to yield an appropriate geopolymer for coating of urea granules.

3.2 Characterization of geopolymers

3.2.1 Structural analysis of geopolymer. Fig. 2(a)–(c) shows the FTIR spectra of the raw fly ash samples (OFA, MFA A, and MFA B) and geopolymers prepared using original and mechanically activated fly ash at varying S : L ratios. In region (i), which is the fingerprint region, OFA, MFA A, and MFA B samples displayed broad bands at wavenumbers of 1005, 1009, and 1023 cm^{-1}, respectively, due to asymmetric and symmetric stretching vibrations of Si–O–T (T = Si or Al) bonds.[44] Siloxane (Si–O–Si) is the major bond that exists in coal fly ash material, while the amount of Si–O–Al is lower.[45] When fly ash reacted with NaOH, polycondensation of Si–O–T bonds occurred, which resulted in the formation of the geopolymer gel.[46] This process leads to the shifting of bands to a lower frequency and the peak narrowing for all geopolymer samples ranging from 968 cm^{-1} to 974 cm^{-1} for OFA (I–V), 966 cm^{-1} to 972 cm^{-1} for MFA A (I–V), and 965 cm^{-1} to 971 cm^{-1} for MFA B (I–V). This shifting is attributed to the structural reorganisation due to the formation of amorphous aluminosilicate geopolymer gel. Double peaks located at a wavelength of 791 cm^{-1}, 776 cm^{-1} (OFA), 792 cm^{-1}, 776 cm^{-1} (MFA A) and 795 cm^{-1}, 774 cm^{-1} (MFA B) are ascribed to the stretching symmetric vibration of quartz (Si–O–Si).[47] For
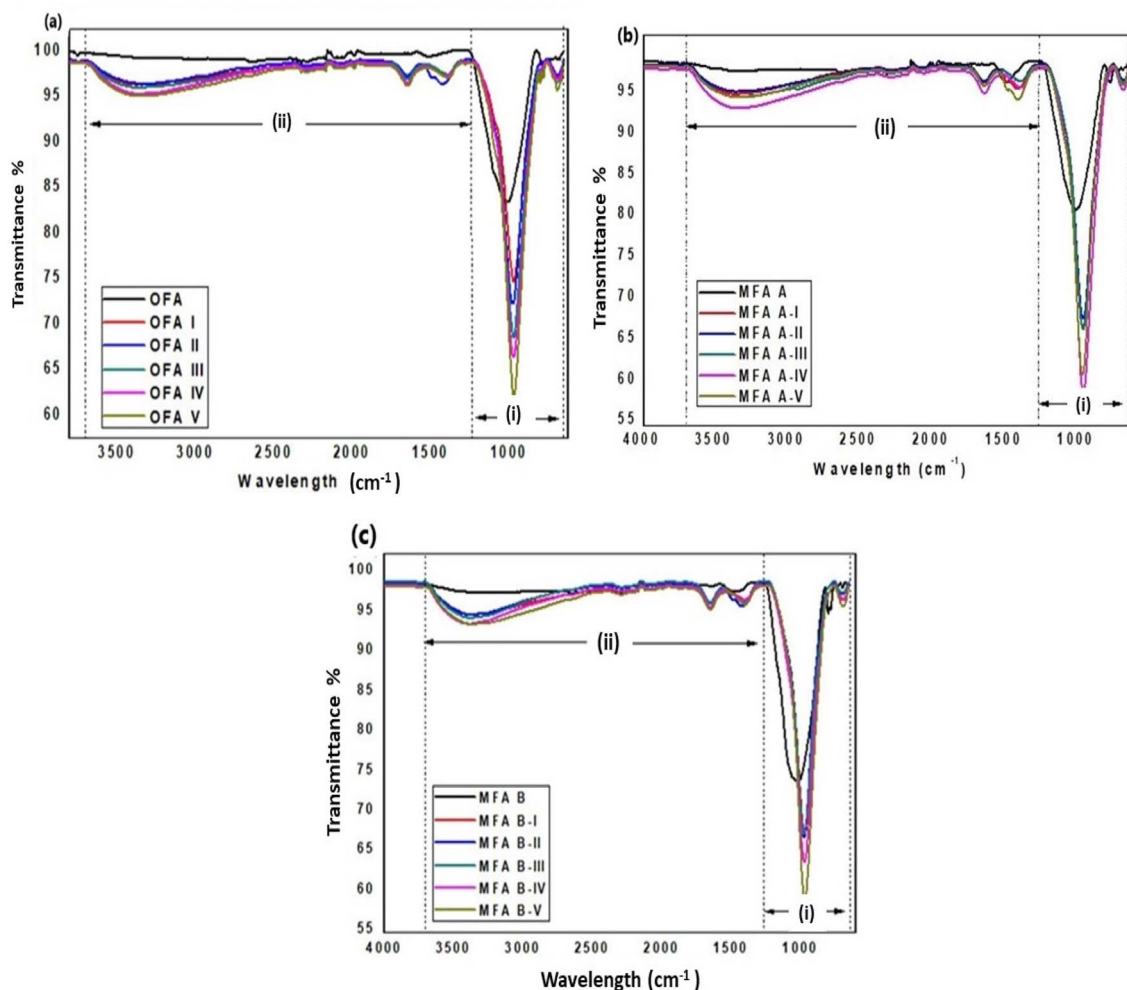

Fig. 2 FTIR spectra of (a) original fly ash (OFA), (b) mechanically activated fly ash (MFA) A and (c) MFA B and geopolymers prepared of those.

geopolymer samples prepared from OFA, only OFA-I, III and V displayed peaks at this region whereas MFA A and MFA B based geopolymer did not show any peaks. Changes in these peaks shows the formation of geopolymer and the decrease in intensity and disappearance of the peaks indicates that the quartz (Si–O–Si) had partially or completely dissolved in the concentrated alkaline solution.[48] Peaks at wavelengths of ∼687 cm^{-1} to 697 cm^{-1} shown in all raw fly ash and geopolymer samples are associated with the bending vibration of Si–O–Al bonds.[49,50]

Furthermore, in the region (ii) other peaks that validate the geopolymer formation are the vibrational broad and intense bands that appear at the wavenumber of ∼3360 to 3390 cm^{-1} and ∼1645 to 1649 cm^{-1} are due to asymmetric vibration of OH stretching and H–O–H bending, respectively.[51,52] These bands are due to bound or atmospheric water molecules that originate from the moisture or water of NaOH solution. Usually most of the water and moisture will evaporate to the atmosphere during curing stage, however they may be also trapped in the cavities of geopolymer matrix.[53] Moreover, it can be observed that the intensity and broadness of the peaks are greater for geopolymer samples (OFA V, MFA A-IV, and MFA B-V) prepared with a lower S : L ratio (2.4 : 1.0 and 2.3 : 1.0), which indicates a higher water retention in the matrix.[48,54]

Geopolymer prepared from a low S : L ratio contained more water. Therefore, the moisture was not evaporated completely and remained in the voids. Besides that, the peaks at the wavelength ranging approximately from 1390 to 1424 cm^{-1} shown in all geopolymer samples were due to stretching vibration of O–C–O from the carbonate formed due to atmospheric carbonation of residual alkalinity.[55] In fly ashes MFA A and MFA B, the intensity of the peaks at 1474 cm^{-1} and 1499 cm^{-1} (i.e., carbonates) was low and it could be related to the presence of calcite.[48]

3.2.2 X-ray diffraction (XRD) analysis. XRD patterns of geopolymer samples are shown in Fig. 3(a)–(c). The formation of geopolymer network for all samples is indicated by the presence of an amorphous hump approximately in the range of 25° to 35° 2θ which is attributed to the structural reorganisation of crystalline phase in fly ash to amorphous phase of geopolymer material.[56] Furthermore, the appearance of new crystalline phase at 14° and 24° 2θ is attributed to hydroxysodalite (Na$_6$(AlSiO$_4$)$_6$·8(H$_2$O)), a zeolitic phase present in all samples. During geopolymerisation, the amorphous gel can be transformed into crystalline zeolites by hydrothermal aging and presence of alkaline conditions.[57,58] Fig. 3(a) shows that the peak of hydroxysodalite at 14° 2θ is intensified from a low peak intensity of OFA-I to a more prominent peak showed by OFA-V sample, which confirms that more zeolitic phase formed at a higher water content. Zeolites are highly porous and may affect the mechanical and physical properties of the geopolymer
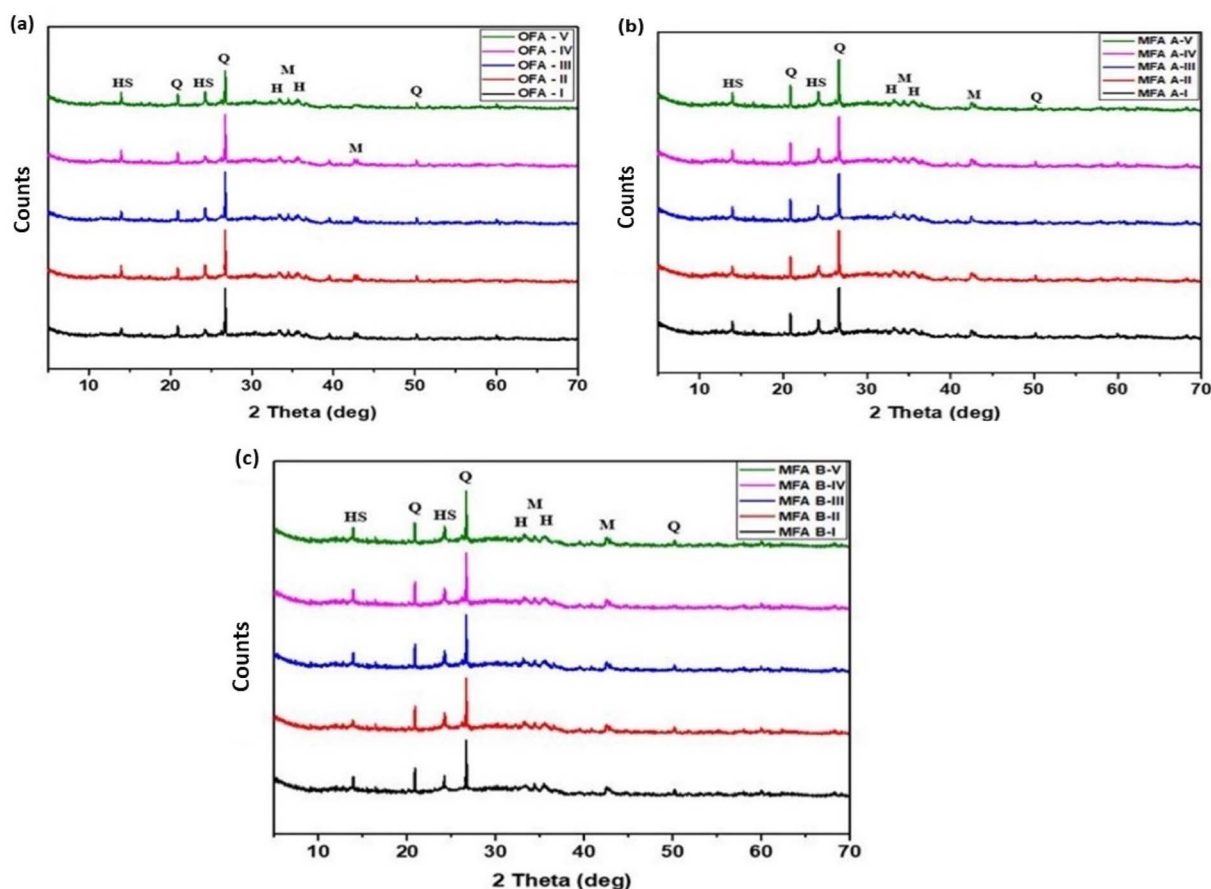

Fig. 3 Diffractograms of (a) original fly ash (OFA), (b) mechanically activated fly ash (MFA) A and (c) MFA B based geopolymers.

samples.[59,60] Crystalline phase found in fly ash such as quartz (Q), mullite (M) and hematite (H) can also be seen in geopolymer XRD pattern owing to their inertness in alkali activation.[46,61]

3.2.3 Setting time. Setting time results of geopolymers are shown in Fig. 4. A low S : L ratio indicates that more water was added into the mix design. All geopolymer samples showed a decrease in setting time when prepared with a high S : L ratio and *vice versa*. For instance, OFA-I with higher S : L (3 : 1) started to set at 35 minutes and fully solidified at 65 minutes. On the other hand, delayed setting was observed for sample OFA-V, which was prepared from the lowest S : L ratio of 2.2 : 1 where the initial and final setting time is 60 min and 115 min, respectively. A similar trend was also displayed by MFA A and MFA B-based geopolymer samples.

The hardening of geopolymer is a result of polycondensation of aluminate and silicate species dissolved from the aluminosilicate precursors and provided by the alkaline activator resulting in the formation of new Si–O–Al and Si–O–Si bonds. Water is merely a medium and do not take part in the reaction as it is released during the polycondensation.[62,63] A high content of water in geopolymer samples prepared from low S : L created gaps that hindered the formation of geopolymer framework of Si–O–Al bonds, subsequently prolonging the hardening process.[49,64] Besides S : L ratio, the particle size of raw material (fly ash) also played a prominent role in the setting behaviour of geopolymer. Rapid setting of geopolymer mixture was observed in the samples prepared from mechanically activated fly ash (MFA A and MFA B) where the fly ash particle is much smaller in size. The shortest initial setting time for OFA based geopolymer was 35 min whereas for MFA A and MFA B-based geopolymer it was 25 min and 10 min, respectively whereby all samples were prepared from a 3 : 1 S : L ratio. Similar pattern was also shown when using low S : L (2.2 : 1) where the MFA B-V sample hardened at the shortest time of 50 min followed by MFA A-V (70 min) and the OFA-V took the longest time to completely harden (115 min).

Fig. 4 Setting time of OFA, MFA A and MFA B based geopolymers.

Table 4 Surface area and pore size analysis results

Geopolymer sample	Physical properties		
	BET surface area ($m^2\ g^{-1}$)	Pore volume ($cm^3\ g^{-1}$)	Average pore diameter (nm)
OFA-I	6.57	0.025	12.53
OFA-II	6.76	0.029	16.49
OFA-III	9.49	0.030	16.26
OFA-IV	10.43	0.046	17.65
OVA-V	15.48	0.067	18.53
MFA A-I	6.53	0.018	12.02
MFA A-II	6.40	0.016	11.98
MFA A-III	7.02	0.02	12.51
MFA A-IV	7.15	0.021	13.70
MFA A-V	10.31	0.023	14.44
MFA B-I	5.40	0.020	9.36
MFA B-II	3.29	0.016	8.75
MFA B-III	3.39	0.013	2.21
MFA B-IV	5.16	0.016	5.80
MFA B-V	7.11	0.022	9.84

3.2.4 Surface area, pore size, and pore volume. The specific surface area, pore size, and pore volume of geopolymer samples are shown in Table 4. BET surface area, pore volume and pore size increases for the OFA-based geopolymer samples with the decrease of S : L ratio which shows that the increase of water content increases porosity. Lowest pore volume for OFA-based geopolymer is shown by OFA-I (0.024 $cm^3\ g^{-1}$) where the sample prepared at the highest S : L ratio. When S : L ratio decreased, the pore volume increased up to 0.067 $cm^3\ g^{-1}$ as shown by OFA-V sample. A similar pattern is also demonstrated for pore sizes. OFA-I showed the smallest average pore size of 12.53 nm whereas the largest average pore size of 18.53 nm was observed for OFA-V. High pore volume and large pore size leads to a much higher surface area. This can be seen from the BET surface area results where increment from 6.57 $m^2\ g^{-1}$ (OFA-I) to 15.48 $m^2\ g^{-1}$ (OFA-V) was obtained. It shows that the increase of water content improves workability of geopolymer paste and increases porosity. When the water or moisture trapped in geopolymer gel evaporates the pores or voids are created. The higher content of water in geopolymer synthesis produces voids or pores.

Geopolymer specimens prepared at the highest S : L ratio for both MFA A and MFA B geopolymers did not show trends like OFA based geopolymers. MFA A-II sample which was synthesised from an S : L ratio of 2.8 : 1 showed a less porous structure where the pore volume (0.01578 $cm^3\ g^{-1}$), average pore diameter (11.98 nm) and BET surface area (6.4 $m^2\ g^{-1}$) were lower than with the MFA A-I sample (S : L= 3 : 1). Nonetheless, for the remaining samples (MFA A-III to MFA A-V), porosity increased with a decreasing S : L ratio where MFA A-V showed the largest value of 0.022 $cm^3\ g^{-1}$, 14.44 nm and 10.31 $m^2\ g^{-1}$ for pore volume, average pore diameter and BET surface area, respectively. As for MFA B based geopolymer (MFA B-I to MFA B-III), the porosity level decreased with a decrease of an S : L ratio. Pore volume and average pore diameter changed from 0.020 $cm^3\ g^{-1}$ to 0.0125 $cm^3\ g^{-1}$ and from 9.84 to 2.21 nm,

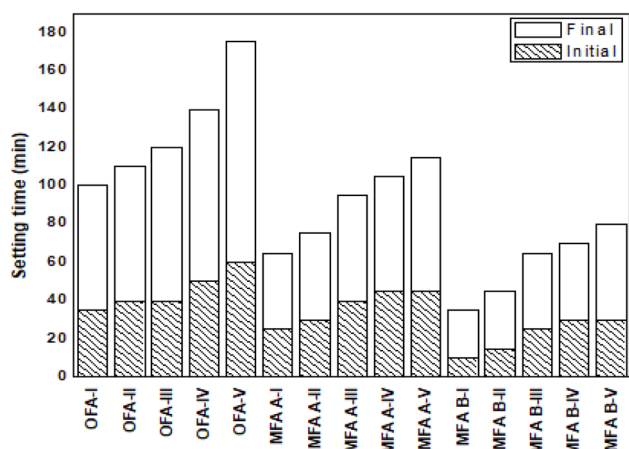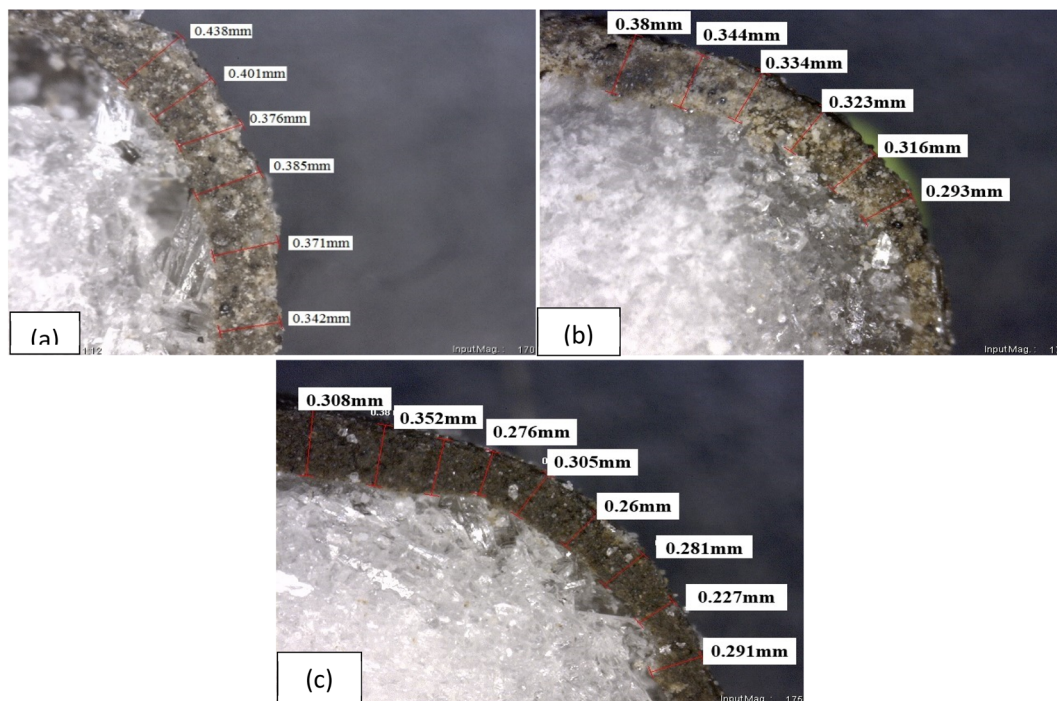Fig. 5   Thickness of unsealed (a) GCU-O (b) GCU-MA and (c) GCU-MB.

respectively. Further addition of water lowered the S : L ratio and affected the surface characteristics where MFA B-IV and MFA B-V showed an increasing pore volume from 0.015 to 0.022 $cm^3 g^{-1}$ and average pore diameter from 5.80 nm to 9.84 nm.

3.2.5   Coating thickness of geopolymer coated urea. Urea coating process involves no chemical reaction between urea and

geopolymer matrix and it is only a physical phenomenon. During the coating process, geopolymer paste was sprayed onto the surface of urea granules. The droplets of sprayed solution were later spread, and they formed a film. Subsequently, solvent (water) present in geopolymer paste evaporated during the oven curing process and produced a dried coating layer. Fig. 5 and 6
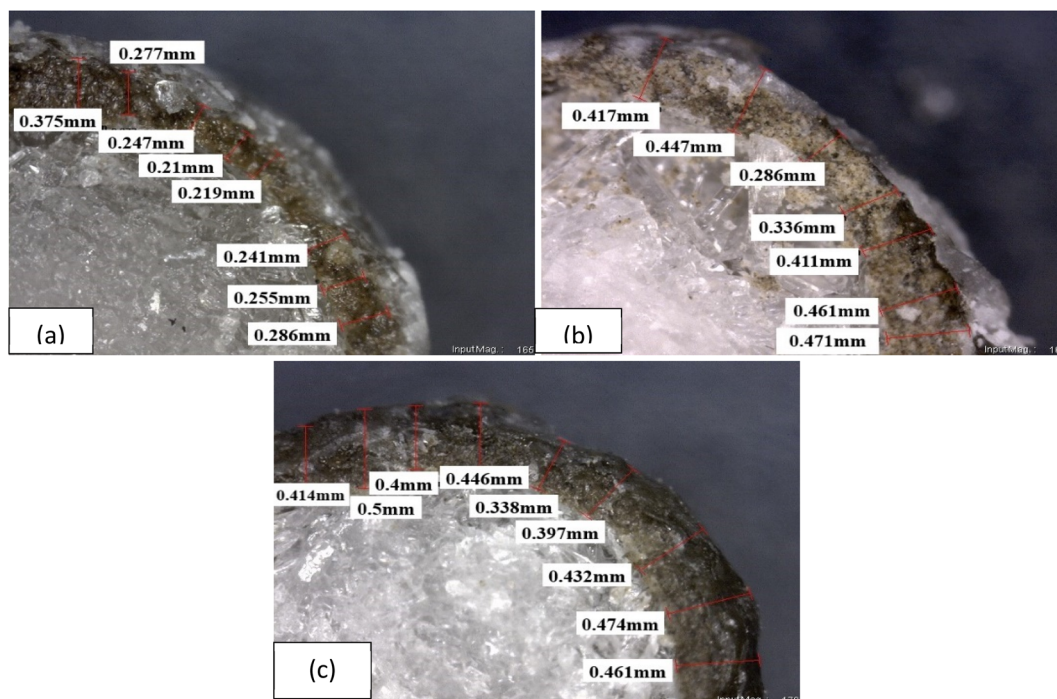
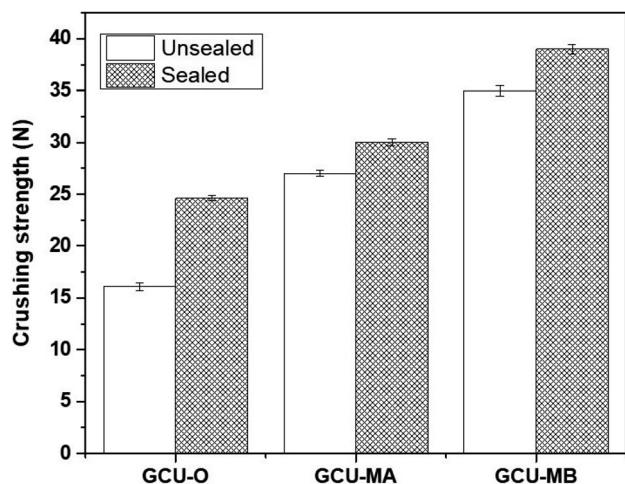Fig. 6   Thickness of sealed (a) GCU-O (b) GCU-MA and (c) GCU-MB.

Fig. 7 Mechanical strength of sealed and unsealed geopolymer-coated urea granules.

non-wax-coated GCU-O, GCU-MA and GCU-MB was 0.369 mm, 0.362 mm, and 0.303 mm, respectively. The use of wax sealant did not affect thickness and resulted in the average thickness of 0.327 mm, 0.363 mm, and 0.379 mm for GCU-O, GCU-MA, and GCU-MB, respectively.

3.3 Crushing strength of geopolymer coated urea

Mechanical properties of coated urea significantly affected its quality and performance. Coated urea is subjected to sudden impact during transportation, storage and handling which usually occur in rough condition. Without sufficient strength, coated urea may undergo mechanical instability that leads to coating layer damage from peeling and attrition.[66,67] The crushing strength of wax-coated and non-wax-coated GCU is shown in Fig. 7. The ability of a material to withstand load is influenced by various factors such as thickness, type, and composition of the coating material. In this stage of the research, a fixed type of coating material (geopolymer), coating thickness (assuming they were the same based on the average thickness calculated in previous section) and GCU granules size were involved.

The crushing strength gradually increased from 16.1 MPa to 27.1 MPa and further to 36.4 MPa with a decreasing particle size for non-wax-coated GCU-O, GCU-MA, and GCU-MB, respectively. Wax sealant was used to fill the pores and voids of geopolymer coating layer substantially enhanced its properties by increasing the crushing strength of all GCU samples which is in agreement with a previous work by Ibrahim *et al.*[68] The range of

display non-wax-coated and wax-coated GCU, respectively. All samples showed a non-uniform film thickness with the coating layer thickness approximately in the range of 0.194 mm to 0.559 mm. The non-uniformity of thickness is due to a variation in the exposure of urea granules to the fresh state geopolymer spray zone. Moreover, contact between coated granules or to the mixing jar walls before curing and drying of the coating film also lead to the uneven film thickness.[65] Average thickness for
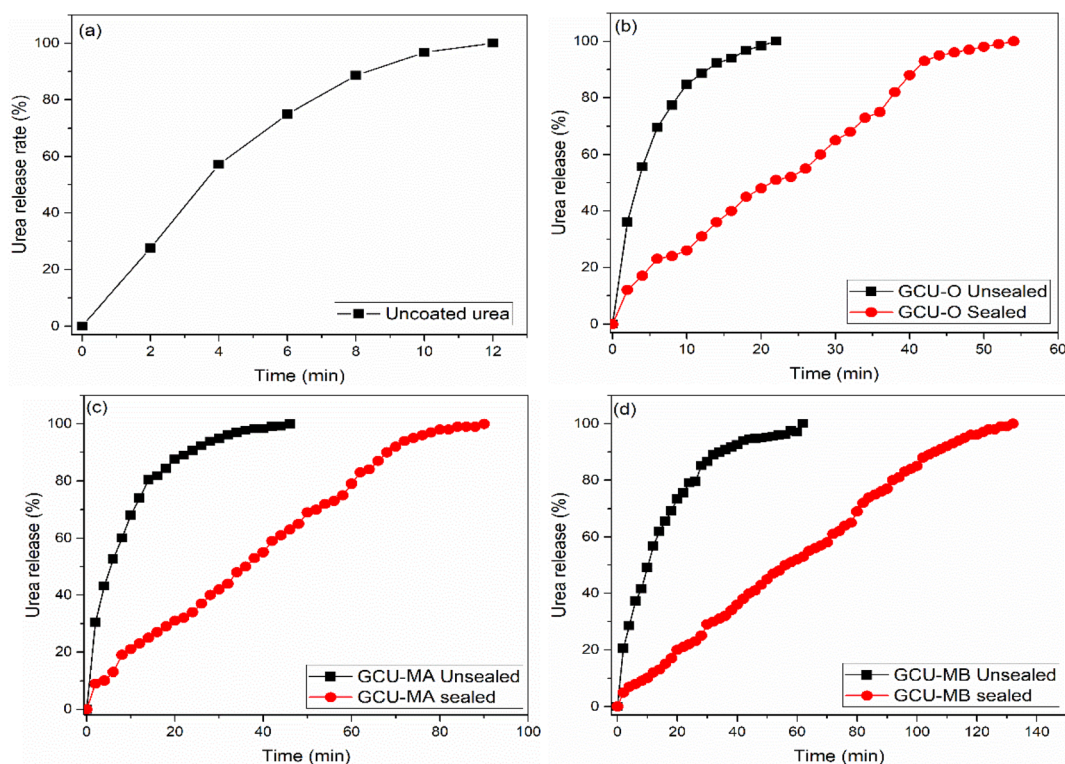

Fig. 8 Release rate of (a) uncoated urea, (b) unsealed and sealed GCU-O, (c) unsealed and sealed GCU-MA and (d) unsealed and sealed GCU-MB in water. Unsealed and sealed samples are without and with wax coating, respectively.
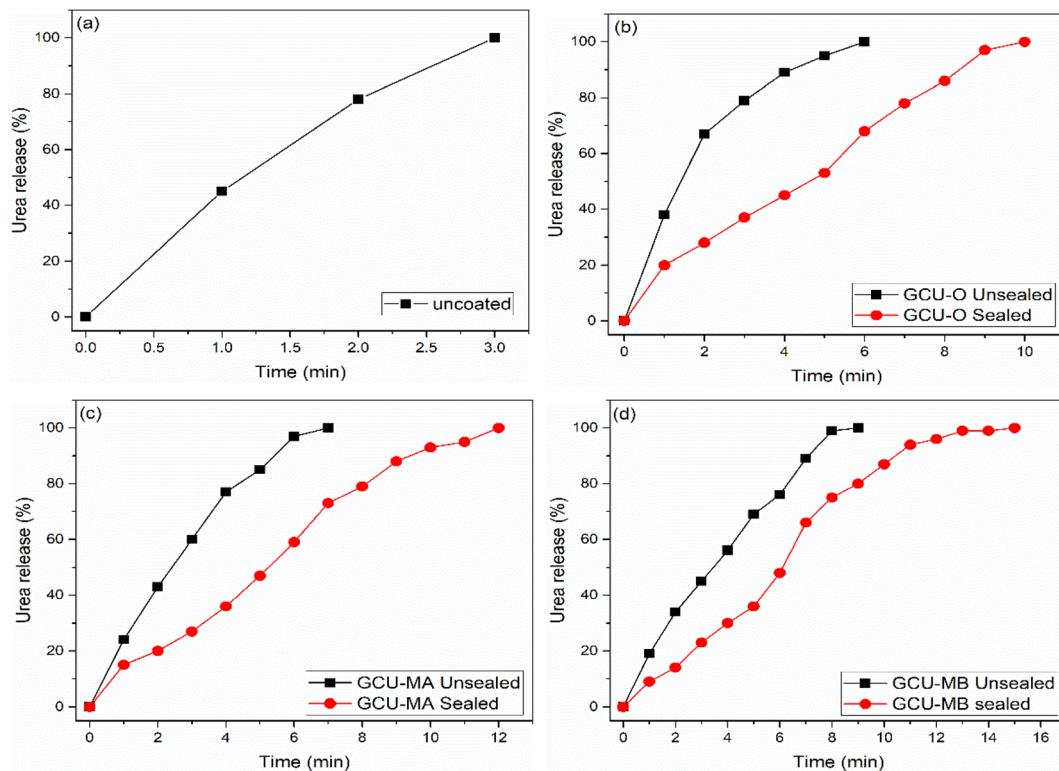
Fig. 9 Release rate of (a) uncoated urea, (b) unsealed and sealed GCU-O, (c) unsealed and sealed GCU-MA and (d) unsealed and sealed GCU-MB in soil.

crushing strength of GCU samples is acceptable when comparing with other coating materials reported in literature, for example crushing strength of biopolymers based coated urea is in the range of 20 to 30 MPa.[69,70] In addition, the crushing strength of sulfur coated urea reported in the literature is ∼17 MPa.[68]

3.4 Urea release profile

3.4.1 Kinetics of urea release in water. Experimental cumulative release of urea in water is shown in Fig. 8. It can be observed that the uncoated urea dissolves rapidly with the shortest release time of 12 min (Fig. 8(a)). Encapsulation of urea with geopolymer showed an improvement in the urea release performance. Non-wax-coated GCU-O showed a complete release at 22 minutes whereas GCU-MA and GCU-MB took 46 and 62 minutes as shown in Fig. 8(b)–(d), respectively. Denser and more compact microstructure of geopolymer with the presence of fewer voids is highly desirable to slow down the release. The increase of thickness of coating material will also delay the release of urea. Moreover, high mechanical strength due to a less porous structure allows the coating film to withstand any sudden load throughout the handling process. Cracking or coating damage due to a rough handling may cause rapid release. The release of urea from sealed GCU is shown in Fig. 8 where sealant (wax) further decreases urea release. The duration of complete nutrient release for sealed GCU-O, GCU-MA, and GCU MB was 54, 90, and 132 minutes respectively.

The voids and pores of geopolymer coating surface were filled and sealed by wax, which resulted in the lower penetration of moisture from outer environment into the urea core and diffusion of dissolved urea to the environment.

3.4.2 Kinetics of urea release in soil. Release of urea from uncoated urea granules and GCU in soil is shown in Fig. 9. The rate of urea release in moist soil environment is slower than in water. The release of urea from uncoated urea occurs fastest with a complete release on the third day after being buried in the soil. Whereas, in Fig. 9(b)–(d), urea granules coated with geopolymer once again exhibited much slower urea release: non-wax-coated GCU-O, GCU-MA and GCU-MB had release of 100% at days 6, 7 and 9, respectively.

Although the complete release of urea from non-wax-coated GCU samples is very close to each other, GCU-MB, which possessed the best coating film properties, demonstrated the slowest release rate. To further delay the urea release, GCUs were sealed with wax, which improved the coating structure and resulted in 100% release within 10 days (GCU-O), 12 days (GCU-MA) and 15 days (GCU-MB) as shown in Fig. 9(a)–(c), respectively. It is worth noting that the release behaviour from sealed GCU-MA and GCU-MB in soil followed the European standard where urea release should not be more than 15% within 24 h.[71]

4. Conclusion

Mechanical activation of fly ash reduced the particle size from d_{50} of 15.3 μm (original size) to 12.0 (MFA A) or 8.6 μm (MFA B).

A low S : L ratio of 2.2 : 1.0 produced a workable and suitable geopolymer coating slurry but it produced a porous geopolymer structure, which is not suitable as a coating material. Geopolymer produced from fine fly ash particles (MFA B-I) hardened rapidly with the setting time of 10 min. Geopolymer prepared using a low S : L ratio (MFA B-V) produced a workable material with enhanced physical and mechanical properties. Geopolymer-coated urea samples prepared using fine fly ash particles and sealed with wax (sealed GCU-MB) had the highest crushing strength of 36.4 MPa and it also significantly prolonged the nutrient release of 100% in 132 min in water and 15 days in soil which was higher than the nutrient release in 12 minutes and 3 days in water and soil, respectively, from uncoated urea. Thus, the geopolymer possess good potential for use as a coating material for urea fertilizer to control its release. Its application as a coating material on other types of fertilizers is an important topic for future studies.

Author contributions

Rashidah Mohamed Hamid: methodology and original draft preparation. Ahmer Ali Siyal: writing – review & editing. Tero Luukkonen: writing – review & editing. Muhammad Rashid Shamsuddin: conceptualization and supervisions. Muhammad Moniruzzaman: supervision and resources.

Conflicts of interest

There are no conflicts to declare.

Acknowledgements

References

1 M. Blois, Expensive inputs and strong demand send fertilizer prices through the roof, available: https://cen.acs.org/business/Expensive-inputs-strong-demand-send/99/web/2021/11, accessed on 18 July 2022.

2 W. Steffen, K. Richardson, J. Rockström, S. E. Cornell, I. Fetzer, E. M. Bennett, R. Biggs, S. R. Carpenter, W. De Vries and C. A. De Wit, Planetary boundaries: guiding human development on a changing planet, *Science*, 2015, **347**, 1259855.

3 N. K. Fageria and M. C. S. Carvalho, Comparison of Conventional and Polymer Coated Urea as Nitrogen Sources for Lowland Rice Production, *J. Plant Nutr.*, 2014, **37**, 1358–1371, DOI: 10.1080/01904167.2014.888736.

4 Comparison: Controlled vs. Slow Release Fertilizer, available: https://www.skspecialties.com.my/controlled-vs-slow-release-fertilizer/.

5 J. O. Chagas, J. M. Gomes, I. C. D. M. Cunha, N. F. S. De Melo, L. F. Fraceto, G. A. Da Silva and F. A. Lobo, Polymeric microparticles for modified release of NPK in agricultural applications, *Arabian J. Chem.*, 2020, **13**, 2084–2095, DOI: 10.1016/j.arabjc.2018.03.007.

6 V. M. Franck, B. A. Hungate, F. S. Chapin and C. B. Field, Decomposition of litter produced under elevated CO_2: dependence on plant species and nutrient supply, *Biogeochemistry*, 1997, **36**, 223–237, DOI: 10.1023/A:1005705300959.

7 D. F. Da Cruz, R. Bortoletto-Santos, G. G. F. Guimarães, W. L. Polito and C. Ribeiro, Role of Polymeric Coating on the Phosphate Availability as a Fertilizer: Insight from Phosphate Release by Castor Polyurethane Coatings, *J. Agric. Food Chem.*, 2017, **65**, 5890–5895, DOI: 10.1021/acs.jafc.7b01686.

8 Z. Ma, X. Jia, J. Hu, Z. Liu, H. Wang and F. Zhou, Mussel-Inspired Thermosensitive Polydopamine-graft-Poly(N-isopropylacrylamide) Coating for Controlled-Release Fertilizer, *J. Agric. Food Chem.*, 2013, **61**, 12232–12237, DOI: 10.1021/jf4038826.

9 A. S. M. Ghumman, R. Shamsuddin, M. M. Nasef, E. G. Krivoborodov, S. Ahmad, A. A. Zanin, Y. O. Mezhuev and A. Abbasi, A Degradable Inverse Vulcanized Copolymer as a Coating Material for Urea Produced under Optimized Conditions, *Polymers*, 2021, **13**, 4040.

10 A. S. M. Ghumman, R. Shamsuddin, M. M. Nasef, C. Maucieri, O. U. Rehman, A. A. Rosman, M. I. Haziq and A. Abbasi, Degradable Slow-Release Fertilizer Composite Prepared by Ex Situ Mixing of Inverse Vulcanized Copolymer with Urea, *Agronomy*, 2022, **12**, 65.

11 Y. Shivay, V. Pooniya, R. Prasad, M. Pal and R. J. C. R. C. Bansal, Sulphur-coated urea as a source of sulphur and an enhanced efficiency of nitrogen fertilizer for spring wheat, *Central Res. Commun.*, 2016, **44**, 513–523.

12 B. Azeem, K. Kushaari, M. Naqvi, L. Kok Keong, M. K. Almesfer, Z. Al-Qodah, S. R. Naqvi and N. Elboughdiri, Production and Characterization of Controlled Release Urea Using Biopolymer and Geopolymer as Coating Materials, *Polymers*, 2020, **12**, 400.

13 W. Suherman and M. Djaeni, Producing Sulfur Coated Urea by Fluid Bed Wet Coating Method: Drying Kinetics and Product Quality, *Int. Rev. Chem. Eng.*, 2010.

14 X. Tong, X. He, H. Duan, L. Han and G. Huang, Evaluation of Controlled Release Urea on the Dynamics of Nitrate, Ammonium, and Its Nitrogen Release in Black Soils of Northeast China, *Int. J. Environ. Res. Public Health*, 2018, **15**, 119.

15 G. Kannan, L. C. Ahmed, B. Duckworth, P. W. Bell and S. K. Subramanian, Coated granular fertilizers, methods of manufacture thereof, and uses, *U.S Pat.*, 10233133, 2019.

16 B. Ni, S. Lü and M. Liu, Novel Multinutrient Fertilizer and Its Effect on Slow Release, Water Holding, and Soil Amending, *Ind. Eng. Chem. Res.*, 2012, **51**, 12993–13000, DOI: 10.1021/ie3003304.

17 Y. Yang, C. Ji, W. Ma, S. Wang, S. Wang, W. Han, A. Mohammat, D. Robinson and P. Smith, Significant soil

acidification across northern China's grasslands during 1980s–2000s, *Global Change Biol.*, 2012, **18**, 2292–2300, DOI: **10.1111/j.1365-2486.2012.02694.x**.

18 P. Lu, Y. Zhang, C. Jia, Y. Li and Z. Mao, Use of polyurea from urea for coating of urea granules, *SpringerPlus*, 2016, **5**, 457, DOI: **10.1186/s40064-016-2120-x**.

19 K. H. Hong, K. W. Oh and T. J. Kang, Preparation of conducting nylon-6 electrospun fiber webs by the in situ polymerization of polyaniline, *J. Appl. Polym. Sci.*, 2005, **96**, 983–991, DOI: **10.1002/app.21002**.

20 X. Wang, S. Lü, C. Gao, X. Xu, Y. Wei, X. Bai, C. Feng, N. Gao, M. Liu and L. Wu, Biomass-based multifunctional fertilizer system featuring controlled-release nutrient, water-retention and amelioration of soil, *RSC Adv.*, 2014, **4**, 18382–18390, DOI: **10.1039/C4RA00207E**.

21 Y. Shen, C. Zhao, J. Zhou and C. Du, Application of waterborne acrylic emulsions in coated controlled release fertilizer using reacted layer technology, *Chin. J. Chem. Eng.*, 2015, **23**, 309–314, DOI: **10.1016/j.cjche.2014.09.034**.

22 J. Behin and N. Sadeghi, Utilization of waste lignin to prepare controlled-slow release urea, *Int. J. Recycl. Org. Waste Agr.*, 2016, **5**, 289–299, DOI: **10.1007/s40093-016-0139-1**.

23 S. Lü, C. Gao, X. Wang, X. Xu, X. Bai, N. Gao, C. Feng, Y. Wei, L. Wu and M. Liu, Synthesis of a starch derivative and its application in fertilizer for slow nutrient release and water-holding, *RSC Adv.*, 2014, **4**, 51208–51214, DOI: **10.1039/C4RA06006G**.

24 J. Chen, S. Lü, Z. Zhang, X. Zhao, X. Li, P. Ning and M. Liu, Environmentally friendly fertilizers: a review of materials used and their effects on the environment, *Sci. Total Environ.*, 2018, **613–614**, 829–839, DOI: **10.1016/j.scitotenv.2017.09.186**.

25 Y. Huang and M. Han, The influence of α-Al_2O_3 addition on microstructure, mechanical and formaldehyde adsorption properties of fly ash-based geopolymer products, *J. Hazard. Mater.*, 2011, **193**, 90–94, DOI: **10.1016/j.jhazmat.2011.07.029**.

26 A. Buchwald, H. D. Zellmann and C. Kaps, Condensation of aluminosilicate gels—model system for geopolymer binders, *J. Non-Cryst. Solids*, 2011, **357**, 1376–1382, DOI: **10.1016/j.jnoncrysol.2010.12.036**.

27 M. Ahmaruzzaman, A review on the utilization of fly ash, *Prog. Energy Combust. Sci.*, 2010, **36**, 327–363, DOI: **10.1016/j.pecs.2009.11.003**.

28 A. A. Siyal, M. R. Shamsuddin and A. Low, Fly ash based geopolymer for the adsorption of cationic and nonionic surfactants from aqueous solution – a feasibility study, *Mater. Lett.*, 2021, **283**, 128758, DOI: **10.1016/j.matlet.2020.128758**.

29 S. K. Kaliappan, A. A. Siyal, Z. Man, M. Lay and R. Shamsuddin, Effect of pore forming agents on geopolymer porosity and mechanical properties, presented at *AIP Conference Proceedings*, 2016, vol. 1, p. 020066.

30 G. Fahim Huseien, J. Mirza, M. Ismail, S. K. Ghoshal and A. Abdulameer Hussein, Geopolymer mortars as sustainable repair material: a comprehensive review,

Renewable Sustainable Energy Rev., 2017, **80**, 54–74, DOI: **10.1016/j.rser.2017.05.076**.

31 A. A. Siyal, R. Shamsuddin, A. Low and A. Hidayat, Adsorption Kinetics, Isotherms, and Thermodynamics of Removal of Anionic Surfactant from Aqueous Solution Using Fly Ash, *Water, Air, Soil Pollut.*, 2020, **231**, 509, DOI: **10.1007/s11270-020-04879-2**.

32 E. D. Rodríguez, S. A. Bernal, J. L. Provis, J. Paya, J. M. Monzo and M. V. Borrachero, Effect of nanosilica-based activators on the performance of an alkali-activated fly ash binder, *Cem. Concr. Compos.*, 2013, **35**, 1–11, DOI: **10.1016/j.cemconcomp.2012.08.025**.

33 C. Ferone, F. Colangelo, G. Roviello, D. Asprone, C. Menna, A. Balsamo, A. Prota, R. Cioffi and G. Manfredi, Application-Oriented Chemical Optimization of a Metakaolin Based Geopolymer, *Materials*, 2013, **6**, 1920–1939.

34 T. Yang, H. Zhu and Z. Zhang, Influence of fly ash on the pore structure and shrinkage characteristics of metakaolin-based geopolymer pastes and mortars, *Constr. Build. Mater.*, 2017, **153**, 284–293, DOI: **10.1016/j.conbuildmat.2017.05.067**.

35 J. Davidovits, Years of successes and failures in geopolymer applications. Market trends and potential breakthroughs, in *Geopolymer 2002 conference*, Geopolymer Institute Saint-Quentin, France and Melbourne, Australia, 2002, vol. 28, p. 29.

36 C. Ferone, G. Roviello, F. Colangelo, R. Cioffi and O. Tarallo, Novel hybrid organic-geopolymer materials, *Appl. Clay Sci.*, 2013, **73**, 42–50, DOI: **10.1016/j.clay.2012.11.001**.

37 R. R. Lloyd, J. L. Provis and J. S. J. Van Deventer, Acid resistance of inorganic polymer binders. 1. Corrosion rate, *Mater. Struct.*, 2012, **45**, 1–14, DOI: **10.1617/s11527-011-9744-7**.

38 A. M. Aguirre-Guerrero, R. A. Robayo-Salazar and R. M. De Gutiérrez, A novel geopolymer application: coatings to protect reinforced concrete against corrosion, *Appl. Clay Sci.*, 2017, **135**, 437–446, DOI: **10.1016/j.clay.2016.10.029**.

39 Y. Ma, G. Ye and J. Hu, Micro-mechanical properties of alkali-activated fly ash evaluated by nanoindentation, *Constr. Build. Mater.*, 2017, **147**, 407–416, DOI: **10.1016/j.conbuildmat.2017.04.176**.

40 M. Olivia and H. Nikraz, Properties of fly ash geopolymer concrete designed by Taguchi method, *Mater. Des.*, 2012, **36**, 191–198, DOI: **10.1016/j.matdes.2011.10.036**.

41 H. Yan, X. Zhu, F. Dai, Y. He, X. Jing, P. Song and R. Wang, Porous geopolymer based eco-friendly multifunctional slow-release fertilizers for promoting plant growth, *Colloids Surf., A*, 2021, **631**, 127646, DOI: **10.1016/j.colsurfa.2021.127646**.

42 X. Zou, D. W. Valentine, R. L. Sanford and D. Binkley, Resin-core and buried-bag estimates of nitrogen transformations in Costa Rican lowland rainforests, *Plant Soil*, 1992, **139**, 275–283, DOI: **10.1007/BF00009319**.

43 B. R. Araújo, L. P. C. Romão, M. E. Doumer and A. S. Mangrich, Evaluation of the interactions between chitosan and humics in media for the controlled release of

nitrogen fertilizer, *J. Environ. Manage.*, 2017, **190**, 122–131, DOI: 10.1016/j.jenvman.2016.12.059.

44 M. B. Ogundiran and S. Kumar, Synthesis and characterisation of geopolymer from Nigerian Clay, *Appl. Clay Sci.*, 2015, **108**, 173–181, DOI: 10.1016/j.clay.2015.02.022.

45 M. Irfan, M. B. Khan Niazi, A. Hussain, W. Farooq and M. H. Zia, Synthesis and characterization of zinc-coated urea fertilizer, *J. Plant Nutr.*, 2018, **41**, 1625–1635, DOI: 10.1080/01904167.2018.1454957.

46 C.-L. Hwang and T.-P. Huynh, Effect of alkali-activator and rice husk ash content on strength development of fly ash and residual rice husk ash-based geopolymers, *Constr. Build. Mater.*, 2015, **101**, 1–9, DOI: 10.1016/j.conbuildmat.2015.10.025.

47 M. J. A. Mijarsh, M. A. Megat Johari and Z. A. Ahmad, Synthesis of geopolymer from large amounts of treated palm oil fuel ash: application of the Taguchi method in investigating the main parameters affecting compressive strength, *Constr. Build. Mater.*, 2014, **52**, 473–481, DOI: 10.1016/j.conbuildmat.2013.11.039.

48 S. Onisei, Y. Pontikes, T. Van Gerven, G. N. Angelopoulos, T. Velea, V. Predica and P. Moldovan, Synthesis of inorganic polymers using fly ash and primary lead slag, *J. Hazard. Mater.*, 2012, **205–206**, 101–110, DOI: 10.1016/j.jhazmat.2011.12.039.

49 S. Mu, J. Liu, W. Lin, Y. Wang, J. Liu, L. Shi and Q. Jiang, Property and microstructure of aluminosilicate inorganic coating for concrete: role of water to solid ratio, *Constr. Build. Mater.*, 2017, **148**, 846–856, DOI: 10.1016/j.conbuildmat.2017.05.070.

50 C. Y. Heah, H. Kamarudin, A. M. Mustafa Al Bakri, M. Bnhussain, M. Luqman, I. Khairul Nizar, C. M. Ruzaidi and Y. M. Liew, Study on solids-to-liquid and alkaline activator ratios on kaolin-based geopolymers, *Constr. Build. Mater.*, 2012, **35**, 912–922, DOI: 10.1016/j.conbuildmat.2012.04.102.

51 M. A. Salih, N. Farzadnia, A. A. Abang Ali and R. Demirboga, Effect of different curing temperatures on alkali activated palm oil fuel ash paste, *Constr. Build. Mater.*, 2015, **94**, 116–125, DOI: 10.1016/j.conbuildmat.2015.06.052.

52 Q. Wan, F. Rao, S. Song, R. E. García, R. M. Estrella, C. L. Patiño and Y. Zhang, Geopolymerization reaction, microstructure and simulation of metakaolin-based geopolymers at extended Si/Al ratios, *Cem. Concr. Compos.*, 2017, **79**, 45–52, DOI: 10.1016/j.cemconcomp.2017.01.014.

53 M. a. B. Abdullah, L. Jamaludin, H. Kamarudin, M. Binhussain, C. R. Ghazali and A. Izzat, Study on fly ash based geopolymer for coating applications, *Adv. Mater. Res.*, 2013, **686**, 227–233.

54 S. Kumar, F. Kristály and G. Mucsi, Geopolymerisation behaviour of size fractioned fly ash, *Adv. Powder Technol.*, 2015, **26**, 24–30, DOI: 10.1016/j.apt.2014.09.001.

55 Z. Yahya, M. M. a. B. Abdullah, K. Hussin, K. N. Ismail, R. A. Razak and A. V. Sandu, Effect of Solids-to-Liquids, Na$_2$SiO$_3$-to-NaOH and Curing Temperature on the Palm Oil Boiler Ash (Si + Ca) Geopolymerisation System, *Materials*, 2015, **8**, 2227–2242.

56 J. N. Yankwa Djobo, A. Elimbi, H. K. Tchakouté and S. Kumar, Mechanical activation of volcanic ash for geopolymer synthesis: effect on reaction kinetics, gel characteristics, physical and mechanical properties, *RSC Adv.*, 2016, **6**, 39106–39117, DOI: 10.1039/C6RA03667H.

57 W. D. A. Rickard, J. Temuujin and A. Van Riessen, Thermal analysis of geopolymer pastes synthesised from five fly ashes of variable composition, *J. Non-Cryst. Solids*, 2012, **358**, 1830–1839, DOI: 10.1016/j.jnoncrysol.2012.05.032.

58 M. Irfan Khan, K. Azizli, S. Sufian and Z. Man, Sodium silicate-free geopolymers as coating materials: effects of Na/Al and water/solid ratios on adhesion strength, *Ceram. Int.*, 2015, **41**, 2794–2805, DOI: 10.1016/j.ceramint.2014.10.099.

59 N. K. Lee, H. R. Khalid and H. K. Lee, Synthesis of mesoporous geopolymers containing zeolite phases by a hydrothermal treatment, *Microporous Mesoporous Mater.*, 2016, **229**, 22–30, DOI: 10.1016/j.micromeso.2016.04.016.

60 Y.-M. Liew, C.-Y. Heah, A. B. Mohd Mustafa and H. Kamarudin, Structure and properties of clay-based geopolymer cements: a review, *Prog. Mater. Sci.*, 2016, **83**, 595–629, DOI: 10.1016/j.pmatsci.2016.08.002.

61 S. Hanjitsuwan, S. Hunpratub, P. Thongbai, S. Maensiri, V. Sata and P. Chindaprasirt, Effects of NaOH concentrations on physical and electrical properties of high calcium fly ash geopolymer paste, *Cem. Concr. Compos.*, 2014, **45**, 9–14, DOI: 10.1016/j.cemconcomp.2013.09.012.

62 A. A. Aliabdo, A. E. M. Abd Elmoaty and H. A. Salem, Effect of cement addition, solution resting time and curing characteristics on fly ash based geopolymer concrete performance, *Constr. Build. Mater.*, 2016, **123**, 581–593, DOI: 10.1016/j.conbuildmat.2016.07.043.

63 T. Rahmiati, K. A. Azizli, Z. Man, L. Ismail and M. F. Nuruddin, The effect of KOH concentration on setting time and compressive strength of fly ash-based geopolymer, *Appl. Mech. Mater.*, 2014, **625**, 94–97.

64 R. H. Abdul Rahim, K. A. Azizli, Z. Man, T. Rahmiati and L. Ismail, Effect of solid to liquid ratio on the mechanical and physical properties of fly ash geopolymer without sodium silicate, *Appl. Mech. Mater.*, 2014, **625**, 46–49.

65 B. Xing, J. D. Eastham and N. P. Wynnyk, Process and apparatus for producing a coated product, *U.S, Pat.*, 8178161, 2012.

66 L. Xie, M. Liu, B. Ni, X. Zhang and Y. Wang, Slow-release nitrogen and boron fertilizer from a functional superabsorbent formulation based on wheat straw and attapulgite, *Chem. Eng. J.*, 2011, **167**, 342–348, DOI: 10.1016/j.cej.2010.12.082.

67 B. Azeem, K. Kushaari, Z. Man and T. H. Trinh, Nutrient release characteristics and coating homogeneity of biopolymer coated urea as a function of fluidized bed process variables, *Can. J. Chem. Eng.*, 2017, **95**, 849–862, DOI: 10.1002/cjce.22741.

68 K. R. Mohd Ibrahim, F. Eghbali Babadi and R. Yunus, Comparative performance of different urea coating materials for slow release, *Particuology*, 2014, **17**, 165–172, DOI: **10.1016/j.partic.2014.03.009**.

69 M. Y. Naz and S. A. Sulaiman, Attributes of natural and synthetic materials pertaining to slow-release urea coating industry, *Rev. Chem. Eng.*, 2017, **33**, 293–308, DOI: **10.1515/revce-2015-0065**.

70 M. Y. Naz and S. A. Sulaiman, Testing of starch-based carbohydrate polymer coatings for enhanced urea performance, *J. Coat. Technol. Res.*, 2014, **11**, 747–756, DOI: **10.1007/s11998-014-9590-y**.

71 H. Bley, C. Gianello, L. D. S. Santos and L. P. R. Selau, Nutrient release, plant nutrition, and potassium leaching from polymer-coated fertilizer, *Rev. Bras. Cienc. Solo*, 2017, **41**, DOI: **10.1590/18069657rbcs20160142**.